6th International Berlin Workshop on
Transport Phenomena with Moving Boundaries
24th-25th November 2011, Berlin, Germany

WIRE BUNDLES AS PACKING ELEMENTS IN SEPARATION COLUMNS

J. GRÜNIG; S.-J. KIM; M. SCHRÖDER; M. KRAUME

- Chair of Chemical and Process Engineering, Technische Universität Berlin, D-13355 Berlin, Germany

Abstract. The wetted wire packing is a concept that promises to have advantages compared to corrugated sheet packings in separation columns. To assess the fluid dynamics and the separation efficiency of the packing, liquid films on single wires and chains were tested in a vertical channel for fluid dynamics and mass transfer. The liquid film flow was characterized by an optical measurement of the local film thickness and bead velocity. To observe the influence of liquid films at neighbouring wires, a wire bundle of 16 wires with a quadratic spacing of 5 mm was also tested. The results showed that the load limits are comparatively high ($F > 6\ Pa^{0.5}$). When assuming a sufficient wire packing density, the separation efficiencies, are in the order of common structured packings but the specific pressure drop is about one order of magnitude lower.

Keywords. Wetted wire packing, mass transfer, fluid dynamics, structured wires

INTRODUCTION

Packed columns are used for various separation problems in the chemical industry. Modern corrugated sheet structured packings (CSSP) offer high separation efficiencies at moderate pressure drop but suffer maldistribution of liquid and gas phase so the liquid has to be redistributed after a certain height.

The concept of the wetted wire packing proposed by Hattori et al. [1] has promise to have a uniform phase distribution in the whole packing and a low specific pressure drop. It mainly consists of parallel wire elements which are individually supplied with liquid from a special liquid distributor. Therefore, the liquid is forced to run on defined flow paths and there is no radial liquid flow which could lead to maldistribution. Chinju et al. [2] and Uchiyama et

al. [3] carried out mass transfer experiments on single wires with the aim to assess the feasibility of wetted wires in packings for the capture of CO_2 from flue gas. Migita et al. [4] performed experiments with a wire bundle of 109 wires in a column with a diameter of 70 mm. A recent study of Pakdehi and Taheri [5] examines a wetted wire packing for the separation of hydrazine from air in a column of 90 mm in diameter and varying packing densities. In all of the above named studies the interaction of the phases at higher gas loads and its effect on the mass transfer was not observed.

This study therefore focuses on the fluid dynamics and mass transfer in the whole gas load range up to flooding condition. The single wire data is then used to estimate the packing performance. To investigate possible interactions between liquid films on neighbouring wires, a wire bundle of 16 wires was also tested.

In previous investigations [6], a single cylindrical wire with a diameter of 1 mm was examined. It revealed that the film features a pattern of liquid beads running over a thin basis film. This raised the question if the bead formation could be suppressed by the wire geometry and how this would affect the fluid dynamics and the mass transfer. Therefore, different chain geometries were observed for their suitability as packing elements.

MATERIALS AND METHODS

The flow sheet of the experimental set-up is shown in Fig. 1. The main element is a vertical glass channel with a quadratic cross sectional area of 20 mm × 20 mm and a length of 1 m. The examined structured wires and chains are fixed in its centre. Water is pumped from a storage tank to the top of the channel. The liquid is distributed on the wire inside the channel top and flows down as a film and gets into contact with the gas phase. At the channel bottom, the liquid is collected and fed back into the storage tank (Fig. 1 a). Air is guided into the bottom of the channel and flows upwards counter currently to the liquid film before it exits into the environment. The inlet temperatures of liquid and gas phase are regulated by heaters and measured at the inlet and outlet of the channel. A high speed camera and a synchronised lighting are used to detect the film thickness at different vertical positions. The analysis of the images is automated with an image recognition software tool. A more detailed description of the test facility and the optical measurement methods is given in Grünig et al. [6]. Different channel head and bottom sections were used for single wire and wire bundle measurements (see Fig. 2). Tab. 1 gives an overview of the properties of the investigated wire geometries.

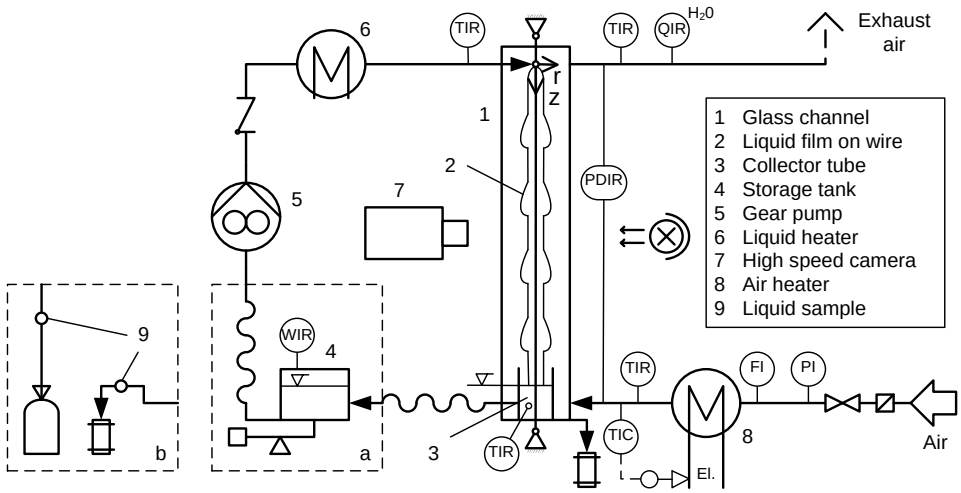

Fig. 1. Sketch of experimental set-up.

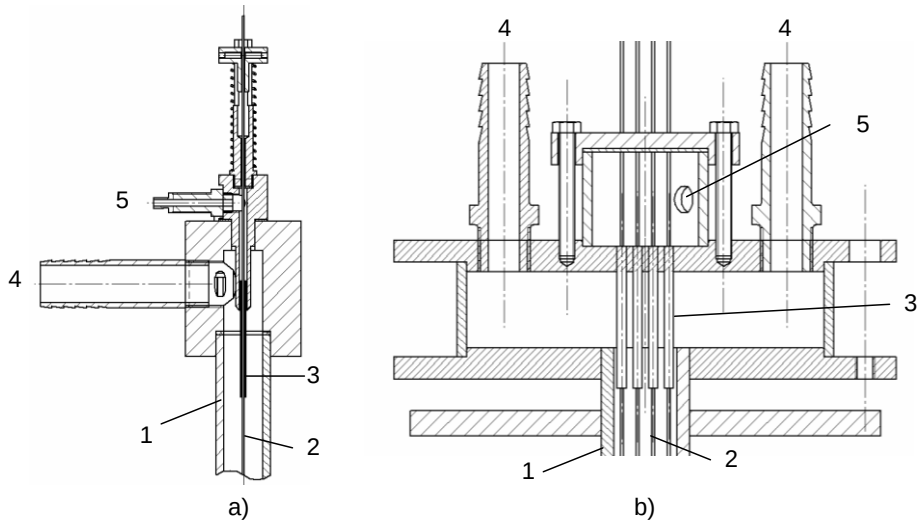

Fig. 2. Construction details of channel head section for a) single wire and b) wire bundle experiments. 1: glass channel, 2: wire (chain), 3: liquid distributor tubing, 4: air exit, 5: liquid inlet.

The gas-side mass transfer was obtained by determining the rate of evaporation from the liquid into the gas phase. A dew point hygrometer is used to measure the humidity of air at the outlet. Before each measurement run the inlet air humidity is measured with the channel under dry conditions.

The liquid-side mass transfer was determined by measuring the desorption of CO_2 from water into air. Water was enriched with CO_2 from a gas bottle. Unlike as for gas-side mass transfer measurements, the liquid was not recycled but drained into a collecting tank (Fig. 1 b). The storage tank was replaced by a 5 L plastic bag so the gas phase could be removed completely.

By this means the desorption of CO_2 from the liquid before entering the channel was avoided. Liquid samples where taken from the inlet and outlet of the channel and were analyzed for their CO_2 concentration.

Tab. 1. Properties of investigated wire geometries.

	Cylindrical wire	Wire bundle Cyl. wires	Watch chain	Armour chain	Bead chain
Material	Stainl. Steel	Stainl. Steel	Brass	Brass	Nickel-pl.
Dimensions, mm			l_1 = 5.6 l_2 = 3.5	l_1 = 3.1 l_2 = 3.8	l_1 = 3.6 d_1 = 2.4
d_W, mm	1	16 × 1	0.8	1	0.6
$\tilde{a}_W$, 10^3 mm^2/m	3.14	50.3	7.10	12.8	5.55
$A_{CSA,W}$, mm^2	0.79	12.6	1.42	3.19	2.13
	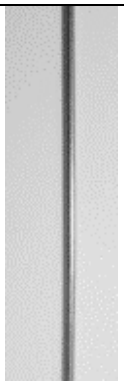	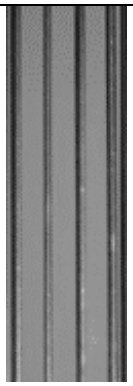	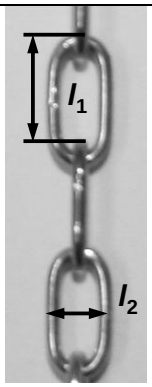	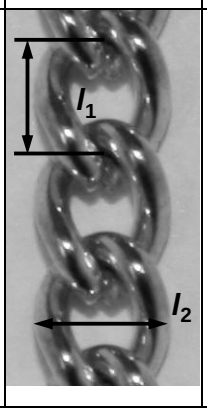	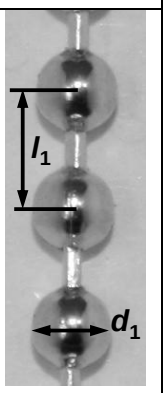

These geometries were chosen since previous investigations revealed that these chains had a desirable effect on the bead motion. The tested wire bundle was an array of 16 round wires (Ø 1 mm) in a quadratic pattern with a pitch of 5 mm. To avoid that liquid was flowing on the channel walls, only the innermost 4 wires were supplied with liquid.

RESULTS

Flow characteristics

Fig. 3 shows images of liquid films on different chain geometries. It revealed that the bead motion could be suppressed by the wire geometry. As can be seen for the watch chain in Fig. 3 a), the beads are embedded in the chain link structure and do not travel downwards. In the case of the bead chain (Fig. 3 b) liquid beads are not observed, but there are liquid streaks

visible which are travelling with low velocity and the film surface is strongly undulated. However, the armour chain (Fig. 3 c) develops a liquid film which is very smooth and no thickness fluctuations can be observed.

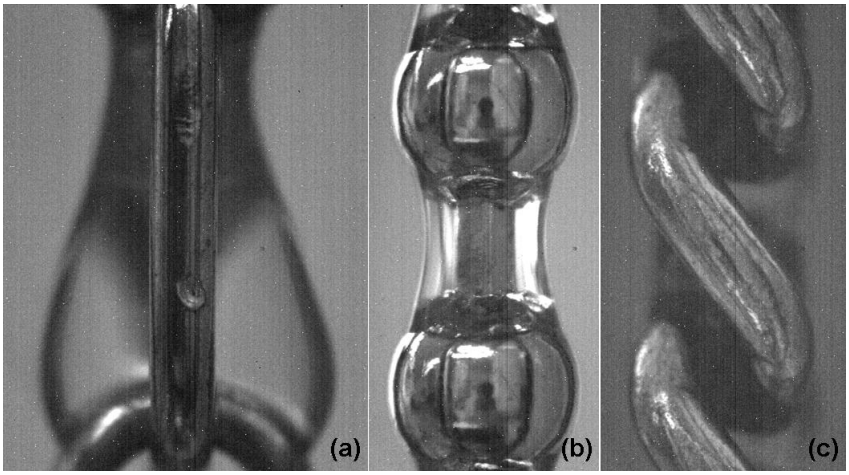

Fig. 3. Liquid film on (a) watch chain (b) bead chain and (c) armour chain.

Load limits

Fig. 4 shows the load limits at the flooding point for different wire geometries. Compared to common structured packings, the load limits of all tested wire geometries are significantly higher. For the armour chain, flooding does occur at very high gas loads which can be explained by the smooth film surface. For all other chains the undulated film surface leads to intensified interaction between the phases and to earlier flooding. It is apparent, that there is a steep increase for the armour chain at low liquid loads. This is caused by the transition from dripping to smooth liquid distribution on the wires. At dripping condition, the liquid is entrained directly from the nozzle whereas at smooth liquid distribution the flooding starts at the bottom of the channel.

Fig. 5 compares the load limits of single wire and wire bundle. When assuming that flooding occurs at the same effective gas velocity, the estimated load limits derived from the single wire data have to be lower since the void fraction and the liquid hold-up are different in the respective configuration. These estimated values have been added to the diagram. It reveals that the measured load limits of the wire bundle are lower than estimated. This indicates that the films on neighbouring wires interfere with each other. As already seen for the armour chain, a dripping liquid distribution lowers the load limits. In the case of the wire bundle, this effect is more pronounced as the liquid distributor tubes have a close distance to each other which means that emerging beads are blocking most of the cross sectional area.

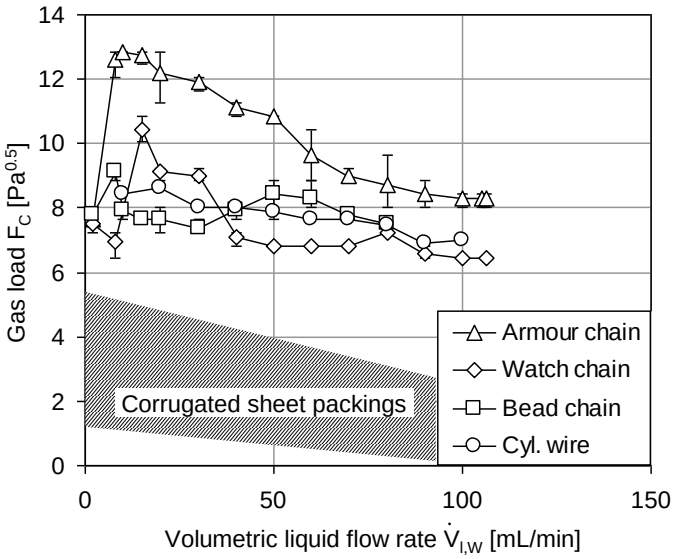

Fig. 4. Load limits at flooding for different single wire geometries.

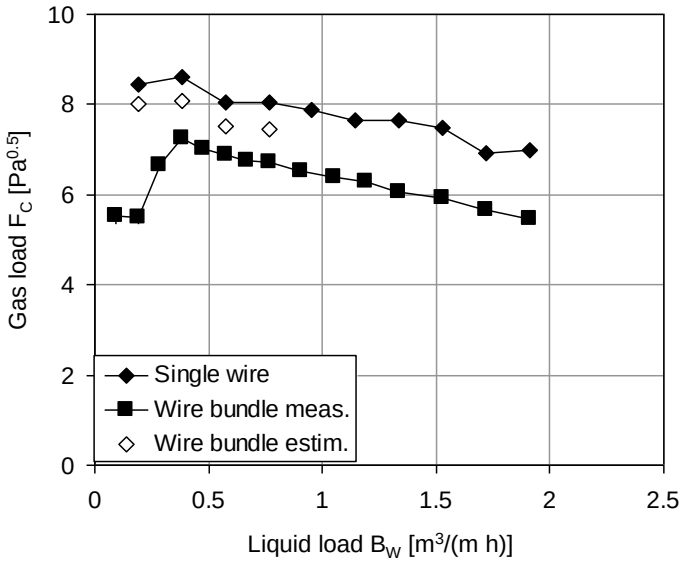

Fig. 5. Load limits for the single wire and the wire bundle. Estimated values for the wire bundle derived from the single wire data considering void fraction and liquid hold-up.

Effective area and mass transfer

The optical film thickness measurements allowed estimating the effective film surface area for mass transfer with a geometrical model of the film (A detailed explanation is given in [6]). Fig. 6 shows the specific effective surface area of different wire geometries depending on the gas load for varying liquid loads. For all wire geometries the effective area does not change with increasing gas load while it increases significantly with rising liquid load. The latter is caused by the strongly curved film surface which increases with rising film thickness. It is

apparent that the effective surface area is enlarged by the chain geometries compared to the cylindrical wire.

In Fig. 7 the gas-side mass transfer coefficients for different wire geometries are plotted against the gas load for different liquid loads. The cylindrical wire effects the highest mass transfer coefficients, followed by the bead chain and the armour chain and the watch chain. The differences can be explained by the bead motion, which enhances the turbulence and thus the mass transfer. It appears that for all wire geometries an increasing liquid load enhances mass transfer which can also be ascribed to intensified interaction of the phases.

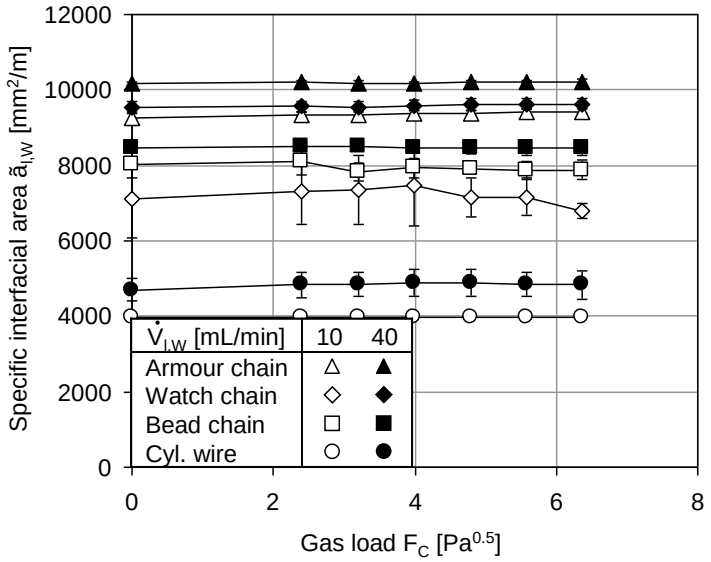

Fig. 6. Specific effective surface area of different wire geometries depending on the gas load for varying liquid loads.

Fig. 8 shows the dimensionless gas-side mass transfer characteristic for the single wire and the wire bundle at different liquid loads which are compared to a correlation for the mass transfer inside structured packings of Bravo et al. [7]. Both configurations were tested in the same range of gas load but since the hydraulic diameter d_h of the wire bundle is lower the Reynolds number are smaller. The results of the wire bundle are slightly higher than those of the single wire measurements which can be explained by more tortuous gas passages between the wires. Compared to the corrugated sheet structured packing correlation, the Sherwood numbers are generally higher. This can be explained by the particular film flow which is characterised by liquid beads which are travelling at high velocity. This enhances mass transfer due to increased turbulence in the gas flow.

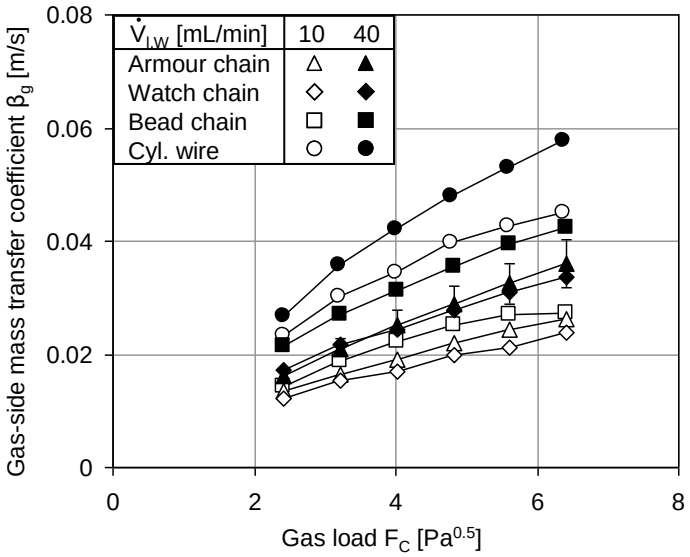

Fig. 7. Gas-side mass transfer coefficient for different wire geometries depending on the gas load for different liquid loads.

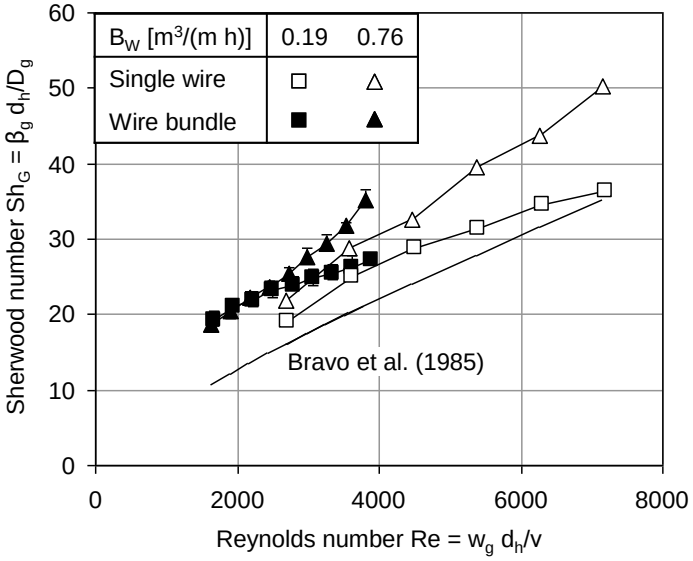

Fig. 8. Dimensionless gas-side mass transfer characteristics for different liquid loads. Comparison of single wire and wire bundle experiments and a correlation for structured packings of Bravo et al. [7].

In Fig. 9 the liquid-side mass transfer coefficients at different liquid loads for single wire and wire bundle configuration are plotted. It appears that the mass transfer coefficients are slightly increasing with rising gas load. When comparing the single wire and the wire bundle data, the values are in good agreement. Unlike for the gas-side mass transfer, there is no influence of liquid films on neighbouring wires on the liquid-side mass transfer which seems plausible.

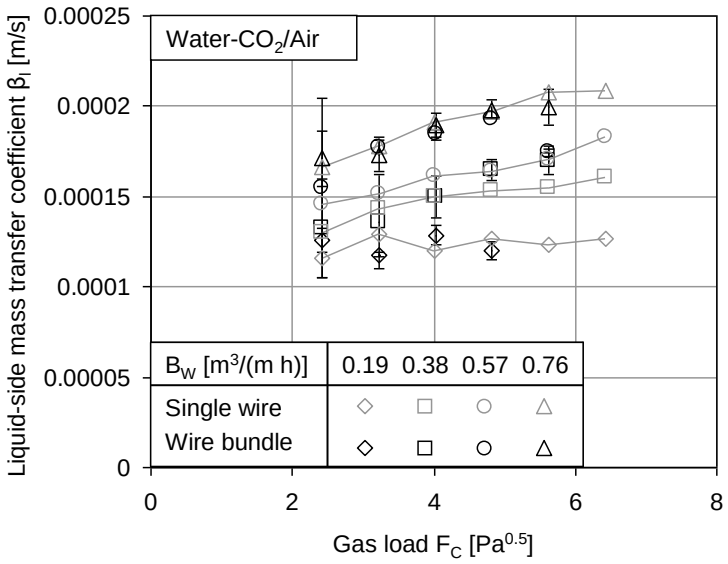

Fig. 9. Liquid-side mass transfer coefficient depending on the gas load for different liquid loads. Comparison of single wire and wire bundle experiments.

Wetted wire packing performance estimation

To achieve a reasonable specific surface area for mass transfer, the wires bundle has to have a certain packing density. If we assume a quadratic pattern of 5 mm spacing, the packing would have a packing density of 40000 wires/m^2 and a specific packing surface area of 125 m^2/m^3. However, when the packing is irrigated, the effective surface area is higher than the dry packing area and can reach up to 200 m^2/m^3 which is comparable to common structured packings. The single wire measurement data was used to estimate the wetted wire packing performance. If we assume equal effective mean gas velocities in both the packing and the channel, the superficial gas velocity in the packing has to be lower. This behaviour is expressed by

$$F_{\mathrm{P}} = \frac{\varepsilon_{\mathrm{P}}(1-h_{\mathrm{l,P}})}{\varepsilon_{\mathrm{C}}(1-h_{\mathrm{l,C}})} F_{\mathrm{C}}\,. \tag{1}$$

The packing liquid load is defined as the total liquid flow rate referred to the cross sectional area of the packing. This means that the flow rate on a single wire has to be multiplied with the packing density:

$$B_{\mathrm{P}} = \dot{V}_{\mathrm{l,W}} z_{\mathrm{P}}\,. \tag{2}$$

Fig. 10 shows the estimated gas-side and the liquid-side separation efficiencies for a wetted wire packing (WWP) with a packing density of 40 000 wires/m^2 expressed by the height of a transfer unit. For comparison, the characteristics for a corrugated sheet structured packing (CSSP) are added to the diagram. The data range reflects the higher operation range of the

wetted wire packing for gas load. The gas-side HTU_g values (Fig. 10 a) are strongly depending on the liquid load which is caused by the fact that the effective surface area as well as the gas side mass transfer coefficients are rising with increasing liquid load.

The higher HTU_g values of the wire packing show that the gas-side separation efficiency is worse than for structured packings of comparable specific surface area. The main reason is that the inclination of the gas channels causes higher effective gas velocities in the corrugated sheet packing. This leads to higher gas-side mass transfer rates compared to the wire packing where the gas passages are straight.

The estimated liquid-side HTU_l values (Fig. 10 b)) are also higher than those of the CSSP but both have a comparable dependency on the liquid load. There is a slight decrease of the HTU_l values with increasing gas load which is due to rising liquid-side mass transfer coefficients (see Fig. 9).

The specific pressure drop of the dry wetted wire packing $(\Delta p/z)_P$ is estimated by a correlation of Rehme [8]. The specific pressure drop of the irrigated packing is calculated with

$$\left(\frac{\Delta p}{z}\right)_{l,P} = \frac{\zeta_{l,P}}{\zeta_P} \frac{1}{(1-h_{l,P})^2} \frac{d_{h,P}}{d_{hl,P}} \left(\frac{\Delta p}{z}\right)_P . \qquad (3)$$

The factor $(\zeta_{l,P}/\zeta_P)$ is replaced by the ratio of friction factors $(\zeta_{l,C}/\zeta_C) = f(F_C, B_W)$ found for the channel by pressure drop measurements. A detailed derivation is given in Grünig et al. [6]. Fig. 11 a) shows the estimated specific pressure drop for the wetted wire packing. It is compared to the model data of Rocha et al. [9, 10]. The predicted specific pressure drop of the wetted wire packing is more than one order of magnitude lower than that of the CSSP. A common measure for the quality of a packing is to plot the pressure drop per transfer unit. In Fig. 11 b) the pressure drop per gas-side transfer unit is plotted against the packing gas load. Although the *HTU* values are worse than those of the CSSP, the wetted wire packing has a pressure drop per transfer unit which is about one order of magnitude lower. This indicates that the wetted wire packing is particularly advantageous for applications which require low specific pressure drops.

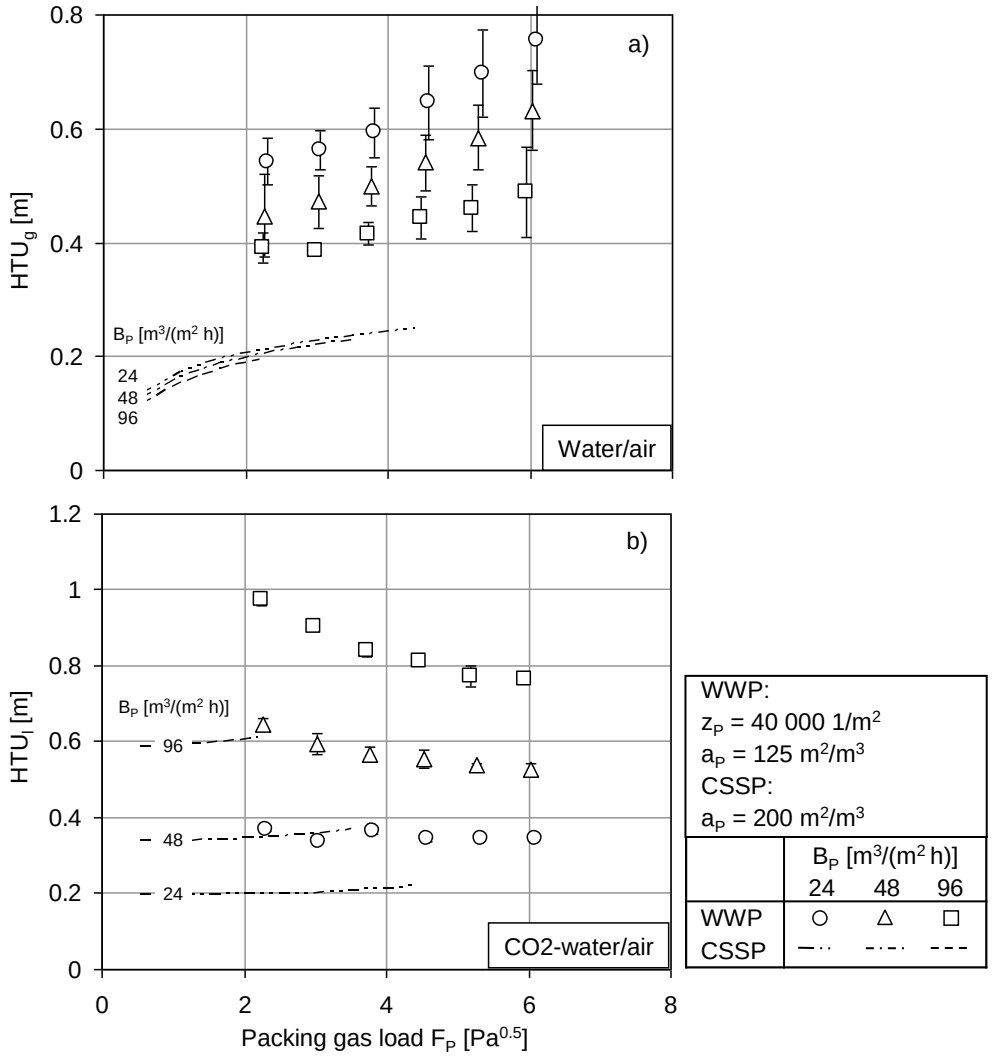

Fig. 10. *HTU* value estimation for a) gas-side mass transfer and b) liquid-side mass transfer depending on the packing gas load for different packing liquid loads for a wetted wire packing. Comparison with a correlation for a corrugated sheet structured packing (CSSP) of Rocha et al. [9, 10].

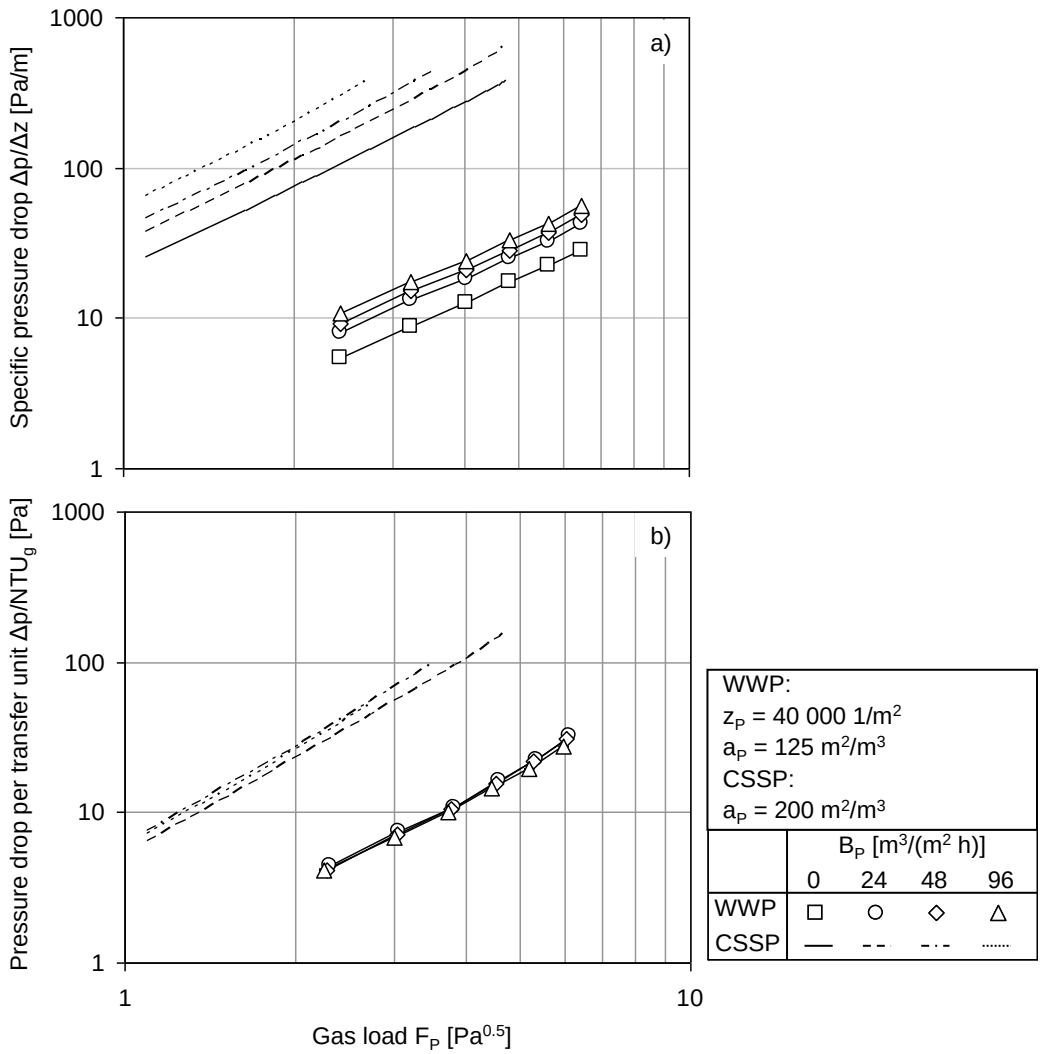

Fig. 11. Estimation of specific pressure drop (a) and pressure drop per transfer unit (b) depending on the gas load for different liquid loads for a wetted wire packing (WWP). Comparison with a correlation for a corrugated sheet structured packing (CSSP) of Rocha et al.[9, 10].

CONCLUSIONS

The results show that liquid beads can be suppressed by appropriate wire geometries. The stabilisation of the film increases the load limits at the cost of reduced mass transfer. An estimation of the wetted wire packing performance indicates that it is strongly depending on the liquid load partly due to the dependency of effective surface area from the liquid load. However, the pressure drop per transfer unit is one order of magnitude lower than of a common structured packing. Provided that the technical challenges can be satisfactorily solved, the wetted wire packing could have significant advantages compared to common structured packings for applications where a low pressure drop is of major concern.

NOTATION

Abbreviations

CSSP Corrugated sheet structured packing

WWP Wetted wire packing

Symbols

A	area, m^2
$a_{l,P}$	specific effective surface area of the packing, m^2/m^3
$\tilde{a}_W$	dry wire area, referred to the wire length, m^2/m
$\tilde{a}_{l,W}$	film surface area on wire, referred to the wire length, m^2/m
a_P	specific surface area of the dry packing, m^2/m^3
$B_W = \acute{V}_{l,W}/C_W$	liquid load of wire, referred to the wire circumference, $m^3/(m\ h)$
$B_P = \acute{V}_l/A_P$	packing liquid load, referred to cross-sectional area, $m^3/(m^2\ h)$
C_W	circumference of wire, m
D	diffusion coefficient, m^2/s
d_W	diameter of wire, m
d_h	hydraulic diameter of the gas passage, m
$F = \nu_g\ \rho_g^{0.5}$	gas load, F-factor, $Pa^{0.5}$
$h_l = V_l/(\varepsilon\ V_{tot})$	liquid fill factor, -
HTU	height of a transfer unit, m
$HU_l = V_{l,W}/L_W$	liquid hold-up, mL/m
L_W	length of wire, m
NTU	Number of transfer units, -
Δp	pressure drop, Pa
$(\Delta p/z)$	specific pressure drop, Pa/m
$Re_g = w_g d_h \rho_g/\eta_g$	Reynolds number of the gas phase, -
$Sc_g = \nu_g/D_g$	gas Schmidt number, -
$Sh_g = \beta_g\ d_h/D_g$	gas Sherwood number, -
s_P	wire spacing in the packing, m
$\acute{V}$	volume flow rate, m^3/s
v_g	superficial gas velocity, m/s
w_g	mean gas velocity, m/s
z	vertical coordinate, m
z_P	packing density of wires per cross-sectional area, $1/m^2$

Greek letters

β	mass transfer coefficient, m/s
δ	film thickness, µm
ε	voidage, -
ζ	friction factor, -
η	dynamic viscosity, Pa s
ρ	density, kg/m^3
σ	surface tension, N/m

Sub- and superscripts

C	channel
g	gas
l	liquid, wetted
P	packing
W	wire

REFERENCES

[1] Hattori, K., M. Ishikawa, and Y.H. Mori: Strings of Liquid Beads for Gas-Liquid Contact Operations. AIChE J., 40 (1994) 12, 1983-1992.

[2] Chinju, H., K. Uchiyama, and Y.H. Mori: "String-of-Beads" Flow of Liquids on Vertical Wires for Gas Absorption. AIChE J., 46 (2000) 5, 937-945.

[3] Uchiyama, K., H. Migita, R. Ohmura, and Y.H. Mori: Gas absorption into "string-of-beads" liquid flow with chemical reaction: application to carbon dioxide separation. Int. J. Heat Mass Transfer, 46 (2003), 457-468.

[4] Migita, H., K. Soga, and Y.H. Mori: Gas Absorption in a Wetted-Wire Column. AIChE J., 51 (2005) 8, 2190-2198.

[5] Pakdehi, S.G. and S. Taheri: Separation of Hydrazine from Air by Wetted Wire Column. Chem. Eng. Technol., 33 (2010) 10, 1687-1694.

[6] Grünig, J., T. Skale, and M. Kraume: Liquid Flow on a Vertical Wire in a Countercurrent Gas Flow. Chem. Eng. J., 164 (2010) 1, 121-131.

[7] Bravo, J.L., J.A. Rocha, and J.R. Fair: Mass-Transfer in Gauze Packings. Hydrocarbon Processing, 64 (1985) 1, 91-95.

[8] Rehme, K.: Simple Method of Predicting Friction Factors of Turbulent-Flow in Non-Circular Channels. Int. J. Heat Mass Transfer, 16 (1973) 5, 933-950.

[9] Rocha, J.A., J.L. Bravo, and J.R. Fair: Distillation-Columns Containing Structured Packings - a Comprehensive Model for Their Performance .1. Hydraulic Models. Ind. Eng. Chem. Res., 32 (1993) 4, 641-651.

[10] Rocha, J.A., J.L. Bravo, and J.R. Fair: Distillation columns containing structured packings: A comprehensive model for their performance. 2. Mass-transfer model. Ind. Eng. Chem. Res., 35 (1996) 5, 1660-1667.